# CHAPTER 1

# Introduction and State of Art

## 1.1 Practical relevance and general description

Microchannels are finding increasing applications in a variety of industrial and medical fields such as in micro-heat-exchangers (e.g., microchannel heat sink, micro-heat pipes etc.) for cooling of electronic components; thermal and pressure sensors for automotive and non-automotive applications; pressure sensors for catheter tips; reactors (lab-on-chip) for separating biological cells; blood analyzers; microducts in infrared detectors, diode lasers, miniature gas chromatographs and high frequency fluidic control systems; micropumps in ink-jet printing, environmental testing and electronic cooling, to name a few. Most of these applications involve convective transport through narrow fluidic confinements, which may be faceted by interesting physical implications. In the following discussions, some important aspects of convective transport through microchannels are highlighted, in particular pertinence to the objective of the present dissertation.

### *1.1.1 Convective transport in microchannels*

Flows through microchannels (i.e. channels having at least one characteristic dimension of order of μm) differ from those through macrochannels in a sense that the flow physics may tend to get altered when the characteristic length scales down from macro to micro (Gad-el-Hak 1999; Gad-el-Hak 2001). The area-to-volume ratio for a device with characteristic length scale of 1.0 m is 1.0 $m^{-1}$, while that for a micro-scale device having a size of 1.0 mm is $10^6$ $m^{-1}$. The million fold increase in surface area relative to volume of the miniaturized device substantially affects the transport of mass, momentum and energy through the surface. In other words, high area-to-volume ratio increases the rate at which the heat escapes and similar arguments can be made regarding mass transfer. It has been established by various experiments that the results with micro-devices may not often be explainable via traditional flow modeling. In a nut shell, it can be conclusively inferred that surface effects dominate in small devices. Such effects may

include boundary slip (Maxwell 1879), thermal creep and temperature jump (Smoluchowski 1898), rarefaction, and special intermolecular interactions (Israelachvili 1991).

Microscale gas flows may have possibilities of deviating from a classical continuum picture in several ways. From a mathematical standpoint, the classical continuum hypothesis is not valid when the distance traversed by molecules between successive collisions (i.e., the mean free path, $\lambda$) becomes comparable with the characteristic length scale (D) of the system over which the changes in the transport phenomena are expected to occur. The ratio of $\lambda$ and D, known as the Knudsen number (Kn = $\lambda/D$), is an indicator of the degree of rarefaction of the system, which determines the extent of deviation from a possible continuum behavior. For $0<Kn<0.001$, the flow domain can be treated as a continuum, in which the Navier-Stokes equations in conjunction with the no-slip wall boundary conditions become applicable. On the other extreme, when $Kn>10$, the flow becomes free molecular in nature, because of negligible molecular collisions. The range of Kn spanning from 0.001 to 0.1 is known as the slip flow regime (Fig. 1.1), over which the no-slip boundary condition becomes invalid, although continuum conservation equations can still be used to characterize the bulk flow. However, over the Kn range of 0.1 to 10 (the so called transitional regime), the continuum hypothesis progressively ceases to work altogether, thereby necessitating a shift of paradigm from the continuum-based modeling to particle-based modeling. Although this classification is based on empirical information and the strict demarcating limits between the different flow regimes may depend on the specific problem geometry (Gad-el-Hak 1999; Beskok and Karniadakis 1999; Beskok et al. 1996), it essentially offers with a qualitative criterion based on which appropriate mathematical models can be chosen for the thermo-fluid analysis, consistent with the underlying physical picture. In this context, it is also important to re-iterate that in micro-scale gas flows, thermodynamic equilibrium may not prevail at the fluid-solid interface. Accordingly, a finite velocity slip and temperature jump may need to be accounted for at the fluid-solid interface (Kennard 1938; Eckert and Drake 1972; Beskok et al. 1996; Gad-el-Hak 1999; Beskok and Karniadakis 1999; Gad-el-Hak 2003). Depending on the degree of

rarefaction of gaseous flows in micro-scale geometries, appropriate physics need to be incorporated in the mathematical model to accommodate these effects. It has been well established by various researchers (Beskok and Karniadakis 1999; Beskok et al. 1996; Karniadakis and Beskok 2002) that the traditional Navier-Stokes equations, coupled with velocity slip and temperature jump conditions at the fluid-solid interface, can simulate gaseous flows in micro-scales to a high degree of accuracy in the slip flow regime. For transition and free molecular flow regimes, however, particle based methods such as the Direct Simulation Monte Carlo (DSMC) need to be adopted (Gad-el-Hak 1999).

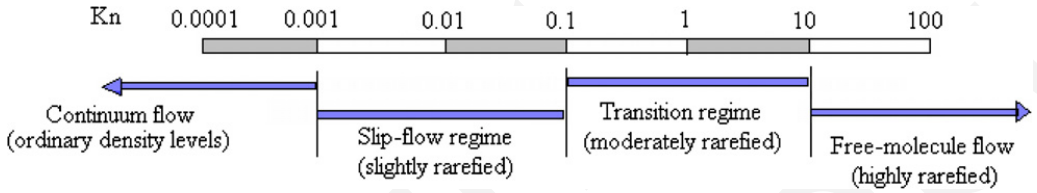


Fig. 1.1: Gaseous flow regimes based on Knudsen number (Kn) (Gad-el-Hak 1999).

Liquid and gas flows obey same equations of motion from a continuum point of view. However, density of liquids is very high in comparison to that of gases. In ideal gases, random molecular motions are responsible for transport processes (such as transfer of molecular momentum) without any role of intermolecular forces. In liquids, molecules are closed packed though not fixed at one position and are always in the state of collisions. Under most circumstances, nevertheless, the incompressible Navier-Stokes equations describe liquid flows, with possible modifications in the boundary treatment. It is also important to mention in this context that for liquids, the concept of mean free path is not very useful and the condition at which liquid flow fails to be in quasi-equilibrium state is not well defined. Also, Knudsen number based classification gets irrelevant for liquids. Nevertheless, liquid flow in microchannel can get significantly affected by interfacial phenomena induced by surface roughness and intermolecular interactions over small scales. Most liquid flows in microchannels come under laminar flow regime because of low Reynolds number hydrodynamics encountered in microfluidic applications. From classical point of view, surface roughness does not influence the laminar flow (Gamrat et al. 2008). However, past works on laminar flow in microchannels (Papautsky et al. 1999; Sobhan and Garimella 2001; Morini 2004; Sharp

and Adrian 2004) have shown significant departures from the classical theory. The possible reasons for these deviations have been attributed to the surface roughness characteristics and wettability (e.g., hydrophobicity or hydrophilicity) conditions that play an important role in microchannel hydrodynamics.

Although the molecular packing in liquids is dense enough to preclude interfacial slip from normal intuitions, slip in liquids is not uncommon. Liquid slip phenomenon may be classified into two categories, namely, real slip and apparent slip. Real slip is the one in which molecular interactions cause an actual relative motion between the fluid molecules and the solid boundary at their points of contact to take place. Real slip in liquids may be possible at very high shear rates (Thompson and Troian 1997), so that liquid molecules may be pulled out of the surface asperities overcoming the attractive interactions. The deviation from no-slip boundary condition may be mathematically represented by a slip length (β), as shown in Fig. 1.2. Considering the slope of the tangent to the velocity profile at the solid boundary, one may write a slip boundary condition using Navier's hypothesis as

$$u_s = \beta \left. \frac{\partial u}{\partial y} \right|_{y=0} \tag{1.1}$$

The slip length, β, in practice, may turn out to be a strong function of the shear rate. The underlying consequence is that a large slip length in liquid flows may be realized when a critical shear rate is exceeded, contrary to common intuitions.

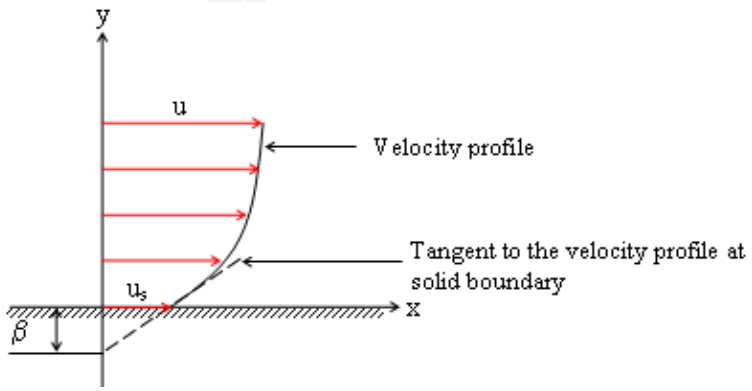


Fig. 1.2: Schematic of real slip and slip length (β).

Apparent slip essentially concerns a modeling paradigm that represents some special interfacial effects in terms of an 'equivalent' slip length, although slip may not occur in reality. A classical example is the case in which surface nanobubbles are formed on fluidic substrates, as attributed to hydrophobic interactions, for instance. The situation may be presented by a schematic as depicted in Fig. 1.3. In Fig. 1.3, a liquid layer flows over a nano-scale bubble matrix of thickness *d*. Because of difficulties in capturing the velocity profile in the ultra-thin less dense (in this case vapor) phase, the liquid velocity profile is traditionally extrapolated to the solid boundary in an effort to represent near-wall flow variations (Tretheway and Meinhart 2004). In doing so, it artificially represents a slip velocity at the interface of liquid-vapor, and a consequent apparent slip length (β) as shown in Fig. 1.3. It is important to mention in this context that the creation of such a depleted phase at the wall would then offer a reduced resistance to the near-wall fluid flow, thus providing the basis for an equivalent slip motion. Such examples may be generalized to state that apparent slip corresponds to the use of fictitious slip conditions to obtain useful models for complicated flow problems, such as those involving liquid flows over vapor layers, grooved plates, and flows of microdisperse liquids. From the viewpoint of continuum mechanics, the apparent slip phenomenon is manifested by strongly non-linear velocity profiles close to the wall, which may not be captured well from experimental conditions, despite using the most sophisticated flow probing techniques available in modern days.

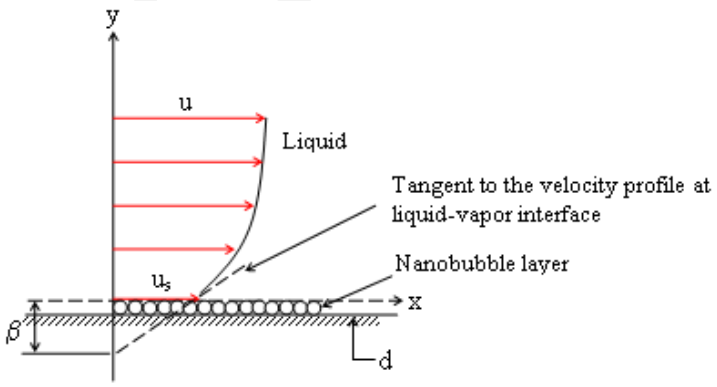


Fig. 1.3: Schematic of apparent slip and slip length (β).

Microscale flows are also faceted by interesting and often non-trivial interfacial interactions. Such interfacial interactions become even more interesting in presence of phase-change phenomena. For example, one may refer to evaporation phenomena from thin liquid films adhering to microchannel walls. Thin film evaporation is one of the effective methods of heat removal from a high heat flux surface for various reasons, including the following: (i) a small quantity of liquid is required for removing the heat by evaporation at the vapor-liquid interface of the thin layer of liquid, (ii) a very high heat transfer coefficient results from the lower thermal resistance across the thin liquid layer, (iii) the substrate experiences a smaller temperature rise above the saturation temperature of the working liquid, as long as a sufficient quantity of liquid is provided to wet the substrate, (iv) a minimum amount of energy is required to circulate the working liquid due to small pressure drop across the thin film evaporator, (v) the upper limit on cooling performance is limited by the kinetics of vapor formation at the vapor-liquid interface. Thin film evaporation phenomenon in microchannel is typically characterized by three broad transport regimes (Wang et al. 2007): namely, the non-evaporating or adsorbed regime, the thin film regime, and the intrinsic meniscus regime as shown in Fig. 1.4. The thin film evaporating region constitutes an extended meniscus beyond the apparent contact line at a liquid/solid interface, which is formed as a combined consequence of the capillary and disjoining pressure effects in the interfacial region. Continuous evaporation of the liquid elements in this region, triggered by the boundary heat flux, may be sustained by a driving pressure gradient that originates from the gradients in the capillary and disjoining pressures. The disjoining pressure represents the change in body force within the liquid due to long range van der Waals forces between the liquid and solid over a narrow range of thickness (Derjaguin and Churaev 1976). It is also defined as a pressure difference across the liquid-vapor interface due to a repulsion of the vapor phase by the solid and the liquid, due to long-range intermolecular forces, in this case van der Waals forces (Schonberg and Wayner 1990). The capillary pressure depends upon surface tension, slope and curvature of the thin film meniscus. The shape-dependent intermolecular force field is used to control the fluid flow and heat transfer. Conversely, transport processes are studied by measuring the temperature field and liquid film shape.

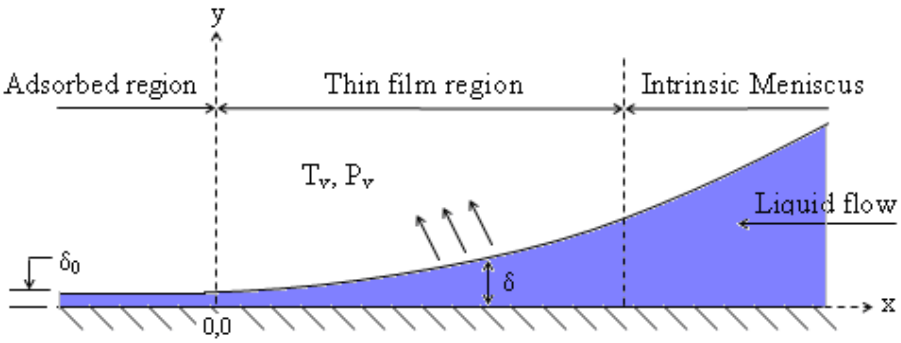


Fig. 1.4: Schematic of an evaporating thin film in a microchannel.

The disjoining pressure, mentioned as above, may also depend on the interfacial topology. For thin liquid films of uniform thickness (δ), the disjoining pressure may be approximated in the leading order to be a function of the film thickness only. However, for varying film thicknesses leading to an asymptotic merging of the liquid with the solid substrate, the disjoining pressure becomes unbounded as $\delta \rightarrow 0$. Hocking (1993) has attempted to rectify this discrepancy by deriving a form of the expression of the disjoining pressure that depends not only on the film thickness, but also on the film slope, based on the earlier developments of Miller and Ruckenstein (1974). However, these derivations have been based on the consideration of constancy of an intermolecular potential on the liquid–vapor interface only, disregarding the requirement of enforcing the same within the inner region of the liquid film as well under equilibrium conditions. Indeikina and Chang (1999) have derived an expression for slope-dependent disjoining pressure, though not rigorously established through the equilibrium constraints. It is also important to mention here that the above modified considerations of disjoining pressure allowed a contact line to move without slip, in clear disagreement with the molecular simulation predictions. In fact, when a liquid film merges on a substrate, an infinite-force singularity likely to result at the contact line of the film is to be moved along the substrate (Dussan and Davis 1974). Origin of this singularity stems from the fact that a fluid particle needs to turn through a finite angle at the contact line within an infinitesimal distance (Dussan 1979). The only mechanism by which this singularity manifested through an unbounded interfacial force may be relieved is through an interfacial slip (Koplik et al. 1989; Thompson and Robins 1989; Barrat and Bocquet 1999; Oron et al. 1997; Shikhmurzaev 1997). However, in the absence of any interfacial slip, such forcing

condition at the interface is clearly unphysical in nature, since it permits the contact line movement even without slip. In an effort to overcome these constraints, Wu and Wong (2004) have derived an alternative expression for slope-dependent disjoining pressure that contained higher order terms (film-curvature dependent), which physically ensured the locking of any contact line motion without slip.

Several other types of interfacial phenomena may become important in microscale applications. However, issues that are not directly relevant to the present scope of investigation are not discussed here, for the sake of brevity.

### 1.1.2 Some practical considerations

The primary focus of this dissertation is the convective transport in microchannels with particular relevance in thermal management of electronic devices. The continuous increase in performance of microprocessors over the past three decades in accordance with 'Moore's Law' (Moore 1975) has called for novel thermal management techniques. In the absence of cooling, the junction temperature of the die of the electronic components reaches a value at which the electronic operation of the device ceases or the component losses its physical integrity, resulting in device failure. Heat is one of the primary sources of electronic hardware failure. Various thermal management techniques (e.g., passive, active, or mixed) are adopted depending upon amount of heat dissipation, size of the device, space availability, reliability and cost. Passive cooling is attractive for low heat flux, simplicity, low cost and high reliability. However their usage is limited only up to few $W/cm^2$ (Ohadi et al. 2005), thus making them inadequate for many high heat dissipating applications.

Air-cooling of electronic components is widely used due to its low cost and simplicity as well as for the fact that air is the ultimate heat sink for most cases. Desktops and notebook computers use air-cooling by free or forced convection over finned surfaces. Liquid cooling and refrigeration cooling techniques have been successfully introduced in high performance computers (Danielson et al. 1986; Vacca et al. 1987; Schmidt 2000). The microprocessors can have an average heat flux of 10-100 $W/cm^2$

(NEMI 2000). High end military and aerospace wide band-gap amplifier, electromagnetic weapons, high power radar electronics and power electronics for hybrid electric vehicle may produce hot spots with heat fluxes on the order of $10^3$ W/cm$^2$ (Mudawar 2001; Ohadi et al. 2002, Ohadi et al. 2003). The existing thermal management techniques may not be able to meet the cooling demands for such extreme high heat fluxes. Table 1.1 shows heat transfer coefficients for various cooling methodologies (Mills 1999).

Table 1.1: Typical values of heat transfer coefficients (Mills 1999)

| Description | Heat Transfer Coefficient, W/(m$^2$·K) |
|---|---|
| Natural convection, air | 3-25 |
| Natural convection, water | 15-1 000 |
| Forced convection, air | 10-200 |
| Forced convection, water | 50-10 000 |
| Condensing steam | 5 000-50 000 |
| Boiling water | 3 000-100 000 |
| Ultra thin film evaporation | 10 000-500 000 |
| Microchannel Cooling | 10 000-1 000 000 |

Natural convection in vertical microchannels can be used for cooling electronic components in consumer and automotive applications. The cost of the cooling budget is less in case of natural convection as it does not need any fan or blower. However, natural convection cooled microchannel heat sink is not efficient for heat load beyond few W/cm$^2$ as pointed out earlier paragraphs and can severely be constrained for higher heat dissipating electronic packages. On the other hand, forced convection liquid cooled microchannel heat sinks are particularly attractive for they are compact, light weight and yet offer large area-to-volume ratio. Higher area-to-volume ratio results in enhanced cooling performance. However, it needs a pump to force liquid through the microchannels. In this context, one may think of using thin film evaporation as a potential tool for cooling of high heat flux devices. Thin film evaporation essentially is a change of phase process of a working liquid that helps to remove a large quantity of heat from a heat dissipating source. Relatively small temperature gradients across the surface can be

achieved with a careful design methodology. The heat is absorbed by the working fluid as heat of vaporization or latent heat. In operation, a temperature gradient forms across the film via heat conduction and the liquid simply vaporizes at the liquid-vapor interface. This process removes a very large amount of heat (Table 1.1) because the amount of heat removed is inversely proportional to the thickness of the thin liquid layer.

## 1.2 State of Art

### *1.2.1 Natural convection in microchannel*

Although a vast body of literature exists on the forced convection gas flows in micro-systems, only a few studies have been reported so far on natural convection in vertical microchannels. Appreciating the technological importance of free convective heat transfer in vertical microchannels, Chen and Weng (2005) have recently presented analytical solutions for velocity and temperature distribution in fully developed natural convection in an open-ended vertical parallel plate microchannel, by taking the velocity slip and temperature jump effects into account. They have also shown that the effects of rarefaction and fluid-wall interaction are to increase the volumetric transport and to decrease the heat transfer rate. Further, it has been established in their study that for fully developed free convection flows with symmetrically heated walls, the Nusselt number turns out to be zero. Such conclusions, however, have been arrived at by neglecting the momentum and heat transfer characteristics in the developing region of the microchannel. On the other hand, in reality, it is expected that the influences of the developing region are likely to alter the free convection heat transfer characteristics in a vertical microchannel to a significant extent. The underling implications might appear to be somewhat intuitive in nature, but are by no means obvious, primarily because of an interesting and non-trivial interplay between the boundary layer growth in the developing region and the micro-scale effects manifested through wall slippage and temperature jump conditions at the gas-solid interface. The situation gets further complicated by the fact that the thermo-physical properties tend to change with changes in temperature, and cannot be taken as constants for the sake of obtaining closed-form solutions of the associated mathematical problem, at the cost of the practical reliability of the model predictions. To the best of the author's knowledge, these issues are yet to be

comprehensively addressed in the context of free convective heat transfer in vertical microchannels.

### *1.2.2 Forced convection in microchannel heat sink*

Tuckerman and Pease (1981) have demonstrated by their pioneering experimental work that the results obtained for laminar flow single-phase water-cooled silicon microchannel heat sink with as low as 50 μm channel width and 300 μm channel depth agrees well with classical predictions. Sobhan and Garimella (2001) have performed an extensive and exhaustive literature survey on friction and heat transfer characteristics for micro-, mini-channels and microtubes with special emphasis on quantitative experimental results and theoretical predictions and have concluded that there is no evidence of violation of continuum assumptions for the microchannels tested most of which have hydraulic diameter of 50 μm or more. Zhang et al. (2005) have conducted experimental and analytical characterization of the thermal performance of heat sink having microchannels of 210 μm width and 2.0 mm depth using single-phase deionized water as coolant and have found good agreement between experiment and analytical results for pressure drop and thermal resistances. Lee, Garimella and Liu (2005) have investigated microchannel heat sink having channels of 194–534 μm width and Reynolds number 300–$3.5\times10^3$ both experimentally and numerically with classical continuum approach. They have found good agreement between experiment and numerical result. Several other researchers (Phillips 1990; Knight et al. 1992; Goldberg 1984; Weisberg et al. 1992; Kim and Kim 1999; Perret et al. 2000; Copeland 2000; Palm 2001; Qu and Mudawar 2002; Ryu et al. 2002; Zhao and Lu 2002; Li, Peterson and Cheng 2004; Li and Peterson 2006; Kim and Kim 2006; Chen 2007; Li and Peterson 2007) also have concluded that Navier-Stokes and energy equations can adequately predict the fluid flow and heat transfer characteristics of microchannel heat sink. The studies outlined above have not focused on the comprehensive effects of all the pertinent design parameters (e.g., aspect ratio of channel, fin thickness or channel width, thickness of heat sink base, number of microchannels, size and location of the heat source on the heat sink, material of the heat sink, and coolant flow rate etc.) on the thermal and hydrodynamic performance of the microchhanel heat sink. Also, there is a lack of a systematic analytical methodology

linking all the design parameters in a common frame-work to characterize the performance of the microchannel heat sink to arrive at an optimum design with superior thermal and low pressure drop system.

### *1.2.3 Thin film evaporation in microchannel*

Comprehensive investigations (Potash and Wayner 1972; Hanlon and Ma 2003; Ma and Peterson 1997) have demonstrated that large increments in the rate of heat transport may be achieved by prolonging the span of the thin film evaporating region. Potash and Wayner (1972), in a pioneering investigation, presented a fundamental model describing an evaporating meniscus that extended beyond the apparent contact line, using the Derjaguin–Landau–Verway–Overbeek (DLVO) theory. Wayner et al. (1976) subsequently pioneered the concept of enhanced capillary transport by employing small-scale grooves, and inferred that thin film evaporation is intensely related to the thermal state of the liquid-vapor interface. Further investigations on thin film evaporation phenomena have been reported in the studies of several researchers in the previous decade (Troung et al. 1987; Wayner 1991; Stephan and Busse 1993; Khrustalev and Faghri 1995; Schonberg et al. 1995; Ma and Peterson 1997). More recently, these considerations have been applied to several other types of geometries as well (Park and Lee 2003; Demsky and Ma 2004; Jiao et al. 2005). Sultan et al. (2005) investigated the effects of Marangoni instabilities on the thin film evaporation process, which may result in a wave-like motion of the interface due to the prevailing temperature gradients. The work of Park et al. (2003) has considered the vapor phase to be saturated in thermodynamic equilibrium with the liquid film. Under this situation, the phase change phenomenon takes place through the mechanism of boiling to maintain saturated temperature at the interface with a wall superheat, the physics of which is entirely different from that of an evaporation transport (Chakraborty and Som 2005). Also, Park et al. (2003) have analyzed the liquid film transport process till such axial length of the film at which the disjoining pressure is greater than or equal to the capillary pressure, thus preventing the thin film region to match the intrinsic meniscus region. In their work, the initial value of curvature ($\delta'' = \left(d^2\delta/dx^2\right)\Big|_{x=0}$) of the liquid film has been set to zero which cannot be specified directly (Wang et al. 2007). Chakraborty and Som (2005), in a

more recent study, have linked the rate of evaporation from the free surface of the thin liquid film into a medium of air and water vapor maintained throughout at a temperature below the saturation temperature corresponding to its existing pressure with the vapor phase mass diffusion. Wang et al. (2007) have investigated an evaporating meniscus in a microchannel through an augmented Young-Laplace equation, by employing a kinetic theory based expression for mass transfer across the liquid-vapor interface. Ma et al. (2008), in another recent investigation, have developed a detailed model to determine the effects of inertial force, interfacial thermal resistance, surface tension, and disjoining pressure on the thin film profile, interfacial temperature variation, fluid flow, and the local heat transfer rates. Do et al. (2008) have developed a mathematical model for predicting the thermal performance of a flat micro heat pipe with a rectangular grooved wick structure. Suman (2008) has investigated the effects of surface-tension gradients on the performance of a micro-grooved heat pipe, through a comprehensive analysis of the underlying thin film evaporation process. The analyses presented in the vast body of literature on thin film evaporation, mentioned as above, have primarily been based on certain simplistic considerations. First, a no-slip boundary condition has been traditionally presumed at the solid-fluid interface, disregarding the underlying details. Secondly, the disjoining pressure for van der Waals force calculation has been traditionally taken to be independent of interfacial slope and curvature, for evaluation of the transport characteristics across the thin film. Clearly, these are likely to be over-simplifications, markedly deviating from physical reality.

## 1.3 Aim and scope of the present work and outline of the thesis

With the consideration to the inferences drawn in the preceding sections, the scope of the present work is designed to be as follows.

### *1.3.1 Natural (gaseous) convection in vertical microchannel*

Aim of this part of the investigation is to execute a comprehensive computational study on free convection heat transfer in the entrance region, followed by that in the fully developed region, in long vertical microchannels with constant wall temperature conditions, for different values of Knudsen number and Rayleigh number, by taking the

temperature-dependent thermo-physical properties into consideration. Both macro-scale (no-slip and no-jump) and micro-scale situations (slip and jump) are studied and compared, so as to develop a thorough physical understanding of the effects of slip and jump conditions on the developing and the developed flows in the microchannel. Special implications of accommodating the effects of the developing region in the heat transfer analysis are discussed in details and important conclusions based on the same are finally pinpointed.

### *1.3.2 Forced (liquid) convection in microchannel heat sink*

Aim of this part of the investigation is to develop a comprehensive and systematic analytical methodology for design and optimization of microchannel heat sinks. The analytical methodology helps to predict transport phenomena (Nusselt number, heat transfer coefficient, total and spreading thermal resistance, and pressure drops) in the microchannel heat sinks with arbitrarily located electronic devices. The footprint of the device is generally smaller than that of the microchannel heat sink. When heat flows from the device to liquid coolant, it encounters various thermal impedances on its path such as internal thermal resistance of the device (known as junction-to-case thermal resistance ($R_{jc}$), interface thermal resistance between device and heat sink ($R_{cs}$), constriction/spreading resistance ($R_{sp}$) (Muzychka et al. 2004), conductive resistance ($R_{con}$), capacitive resistance ($R_{cap}$) and fin resistance ($R_{fin}$). While the two formers ($R_{jc}$ and $R_{cs}$) are external to the heat sink, the latter fours ($R_{sp}$, $R_{con}$, $R_{cap}$, and $R_{fin}$) are internal to the heat sink and are addressed in this work.

### *1.3.3 Thin film evaporation in microchannel*

Aim of this part of the investigation is to characterize thin film evaporation in a microchannel with different values of superheat, and microchannel size. The mathematical model is based on the conservation equations for momentum, mass and heat transport in the liquid phase linked to the vapor phase through the interfacial equilibrium constraints. Augmented Young-Laplace equation (Wayner et al. 1976) is used for predicting the pressure difference, due to capillary and disjoining pressure, between vapor and liquid at the liquid-vapor interface. Mass transfer across the liquid-

vapor interface is predicted using the original equation of Schrage (1953) without any simplification. Equilibrium vapor pressure corresponding to the liquid-vapor interface temperature is calculated accounting the effect of disjoining and capillary pressure (Faghri 1995). Using the semi-analytical formalism developed in this work; local film thicknesses, disjoining and capillary pressure, equilibrium vapor pressure corresponding to liquid-vapor interface temperature, heat flux, and heat transfer coefficient are predicted. Finally, the importance and usefulness of an evaporating thin film for high heat dissipating applications (e.g., 1 000 $W/cm^2$) is delineated.

***Thin film evaporation with slope- and curvature-dependent disjoining pressure:*** Aim of this part of the study is to investigate the thermo-physical transport phenomena in thin liquid films by considering slope- and curvature-dependences of the disjoining pressure, in addition to its traditional dependence on the local film thickness. A comprehensive mathematical model is developed in this regard and is numerically solved, in an effort to determine the interfacial profile in the thin film region and to predict the rate of interfacial heat transfer. Contrasting predictions from the present model and the traditional models considering slope- and curvature-independent disjoining pressures are also pinpointed, so as to reveal the consequences of the underlying micro-scale transport mechanisms on the thin film interfacial profile as well as the pertinent thermo-fluidic characteristics.

***Thin film evaporation with apparent slip:*** Aim of this part of the study is to assess the implications of apparent slip on thin film evaporation phenomenon in a microchannel. The origin of this apparent slip may be the formation of a less dense or depleted phase of nanoscopic span that separates the liquid from the solid boundary. The concerned mathematical model is based on the conservation equations for heat, mass and momentum transport in the liquid phase, linked through the interfacial equilibrium constraints and the apparent slip effects due to depleted gas layer at liquid-wall interface. Following the semi-analytical formalism developed in this work, local film thicknesses is predicted along with the heat and mass transfer variations in terms of the pertinent

dimensionless controlling parameters, revealing the critical consequences of apparent slip on the resultant transport mechanisms.

***Thin film evaporation with real slip:*** Aim of this part of the study is to assess the effect of real slip on thin film evaporation transport process in a microchannel. The real slip phenomenon may stem from a high shear rate that prevails in the thin film region. Leaving apart this contrasting aspect of the origin of slip from the case with apparent slip, other aspects of the mathematical modeling and numerical simulation for this case are similar to the considerations invoked for the case with apparent slip.

Outline of the remaining part of the thesis is organized as follows:

- ***Chapter 2***: Natural convection in vertical microchannel is addressed numerically by two-dimensional Navier-Stokes and energy equations with first order velocity slip and temperature jump at fluid-solid interface.
- ***Chapter 3***: Forced convection in microchannel heat sink is studied semi-analytically for both developing and developed flows with various design parameters and validation is performed with reported experimental data.
- ***Chapter 4***: Thin film evaporation is solved semi-analytically for different superheats, and channel size, and transport phenomena of the thin film is elucidated through the various output parameters that helped to develop a comprehensive fundamental knowledge on evaporating thin film physics. Thin film evaporation with slope- and curvature-dependent disjoining pressure, apparent slip, and real slip is studied and their contrasting effects are elucidated.
- ***Chapter 5***: Concluding remarks are presented.
- ***Chapter 6***: Scope of future work is outlined.